Downloaded from rsta.royalsocietypublishing.org

PHILOSOPHICAL TRANSACTIONS OF THE ROYAL SOCIETY A
MATHEMATICAL, PHYSICAL & ENGINEERING SCIENCES

Probing Semiconductor Interfaces by Transmission Electron Microscopy

J. W. Steeds and D. Cherns

Phil. Trans. R. Soc. Lond. A 1993 **344**, 545-556
doi: 10.1098/rsta.1993.0107

Email alerting service Receive free email alerts when new articles cite this article - sign up in the box at the top right-hand corner of the article or click **here**

To subscribe to *Phil. Trans. R. Soc. Lond. A* go to:
http://rsta.royalsocietypublishing.org/subscriptions

This journal is © 1993 The Royal Society

Downloaded from rsta.royalsocietypublishing.org

MATHEMATICAL, PHYSICAL & ENGINEERING SCIENCES
THE ROYAL SOCIETY A
PHILOSOPHICAL TRANSACTIONS OF

Probing semiconductor interfaces by transmission electron microscopy

By J. W. Steeds and D. Cherns
H. H. Wills Physics Laboratory, University of Bristol, Tyndall Avenue, Bristol BS8 1TL, U.K.

The aim of this article is to review the many available techniques in transmission electron microscopy, drawing attention to their particular characteristics and strengths. Where techniques are well established, the reader is referred to standard reference texts. Greater detail is given about new and emerging techniques which hold promise for even more detailed future study of semiconductor interfaces.

1. Introduction

Transmission electron microscopy (TEM) is a well-established method for study of semiconductor interfaces. The range of available techniques is increasing steadily and the subtlety and complexity of their implementation is growing rapidly. It is not easy for someone new to the field to gain a thorough appreciation of what can be achieved. Here, we attempt to introduce the interested reader to the current state of the art for interfacial studies and to draw attention to important recent developments.

Although TEM and electron diffraction were used in the first elucidation of the 7×7 surface reconstruction of {111} Si specimens, we take the view that TEM is generally used as a technique for studying the interior of thin specimens. This contrasts with the rich variety of scanned surface probe microscopies now emerging. To a very good first approximation the high energy electron beam presents an image which is a projection of the internal structure of the specimen along the beam direction. It is the averaging process involved when projecting along columns of atoms aligned with the electron beam which explains the high quality of many high resolution TEM images as compared with their tunnelling microscopy counterparts. However, we wish to emphasize in this article that the TEM can be used to perform many forms of analysis and imaging in addition to high resolution imaging.

2. High resolution electron microscopy

Semiconductor multilayer structures have been studied extensively in cross section in the TEM with the growth plane approximately edge-on to the electron beam. For near-atomic resolution, samples should ideally be less than 10 nm thick and parallel-sided. This can be achieved by sectioning (often by cleavage) and glueing slices together in the desired orientation. The composite sample is then polished mechanically, preferably with dimpling, to thicknesses of 50 μm or less before finally ion-thinning to perforation.

Phil. Trans. R. Soc. Lond. A (1993) **344**, 545–556
Printed in Great Britain
© 1993 The Royal Society

The Royal Society is collaborating with JSTOR to digitize, preserve, and extend access to *Philosophical Transactions: Physical Sciences and Engineering.* www.jstor.org

Downloaded from rsta.royalsocietypublishing.org

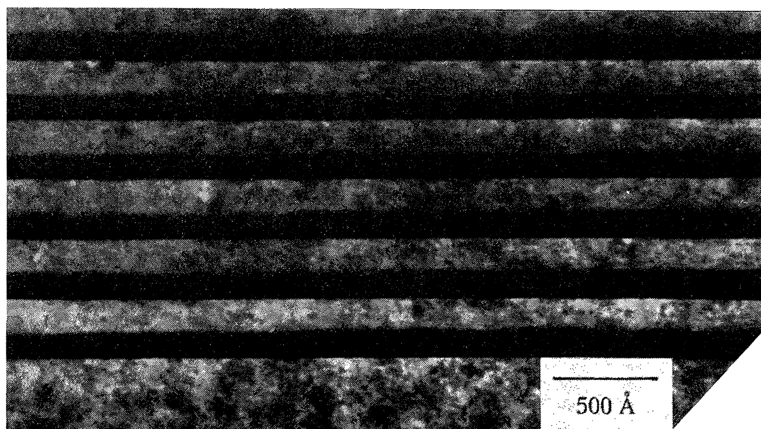

Figure 1. Dark field images in $g = 200$ of an $In_{0.53}Ga_{0.47}As/InP$ cross section. The growth direction is upwards and the InP layers are in strong contrast. (Courtesy of I. K. Jordan, unpublished work.)

Dark field images taken in $g = 200$ are commonly used to profile composition in semiconductor heterostructures. The 200 reflection in diamond and zinc blende structures is 'structurally-sensitive', with a structure factor given by

$$F_{200} = 4[f_A - f_B], \tag{1}$$

where f_A and f_B are the structure factors for atoms on the two FCC sublattices. Figure 1 shows a 200 dark field image of an $In_{0.53}Ga_{0.47}As$–InP structure. The InP 200 structure factor is about five times greater than that of $In_{0.53}Ga_{0.47}As$ and InP appears in much stronger contrast. The image shows quite clearly that the growth of the $In_{0.53}Ga_{0.47}As$ and InP layers leads to alternate roughening and smoothing of the growth surface on a scale of a few tens of nanometres.

Two hundred dark field images have been used to detect layers only one atom layer thick in favourable cases. However, the spatial resolution, d_{min}, which determines the image sharpness, is limited by the size of the objective aperture needed to select a single diffracted beam. Aperture limited resolution is given by $d_{min} \approx u^{-1}$ where u is the range of spatial frequencies transmitted by the aperture. In practice $d_{min} \approx 0.5$–1.0 nm for dark field imaging. To achieve higher spatial resolution it is necessary to use a larger objective aperture which can include several diffracted beams, as in the lattice imaging method. Spatial resolution is then limited by electron optics expressed through the contrast transfer function (CTF) (see Spence 1981). This gives a point resolution, given approximately by the first zero in the CTF ($\sin \chi$) at Scherzer defocus, down to about 0.18–0.20 nm in current high resolution microscopes.

Lattice imaging of semiconductors is usually carried out in the $\{110\}$ projection. Under conventional imaging conditions (Scherzer defocus) $\{110\}$ lattice images are usually dominated by the strong structure-insensitive $\{111\}$ reflections representing a spatial period *ca.* 0.31–0.35 nm, making interfaces difficult to distinguish. This problem is exacerbated by the inability to resolve the projected *ca.* 0.14 nm separation of the two FCC sublattices. Recent progress has been made using non-conventional imaging conditions for particular applications of the technique. Figure 2 shows a $\{110\}$ lattice image of a ZnTe–GaSb interface imaged at an overfocus of 56 nm. Under these conditions the CTF suppresses the contribution of the strong $\{111\}$ reflections to the contrast and enhances reflections near the $\{\frac{1}{2}\frac{1}{2}\frac{1}{2}\}$ positions. The

Downloaded from rsta.royalsocietypublishing.org

Figure 2. (110) lattice image of a ZnTe–GaSb interface at a defocus of +56 nm. A new phase believed to be Ga_2Te_3 is arrowed. (Courtesy of C. T. Chou, unpublished work.)

result is that a new phase, believed to be Ga_2Te_3 (Chou *et al.* 1993) and formed by interface interaction, is clearly visible, whilst at the Scherzer defocus the new phase is virtually undetectable. The new phase is separated by about 5 nm from the original interface, suggesting significant out-diffusion of Ga.

Chemically sensitive lattice images can also be obtained in the {100} projection. In this case the two FCC sublattices are separated by about 0.20 nm, which is resolvable. Ourmazd *et al.* (1989) showed that {100} lattice images, formed by interference between the straight-through beam and four {200} reflections, are chemically sensitive and can be used to profile GaAlAs–GaAs interfaces on an atomic scale.

3. Convergent beam electron diffraction (CBED)

By performing electron diffraction experiments with a small focused probe a wealth of accurate crystallographic information can be obtained concerning semiconductor interfaces. Since the applications of the technique go back over nearly 20 years the interested reader is referred to standard reviews (Steeds 1979; Steeds & Morniroli 1992; Sung 1991; Williams *et al.* 1992). The first application to semiconductor interfaces known to us was published in 1976 (Rackham & Steeds). Information can be obtained readily about lattice parameter changes, composition changes, interface interactions, polarity, disorder, bonding charge distributions, and specimen thickness. The spatial resolution achievable is dependent on the smallest probe size attainable and the broadening which occurs during propagation through the specimen. It is normal (but not essential) to perform CBED experiments on rather thicker specimens than those used in HREM and the technique generally provides a large number of results in a short time. For accurate lattice parameter determination rather thick specimens may be required (just as many lines are required on a high resolution diffraction grating) and this will lead to considerable beam broadening. A typical probe size for these experiments would be 10 nm and broadening might increase this up to around 50 nm in thick specimens. Contamination and radiation

Downloaded from rsta.royalsocietypublishing.org

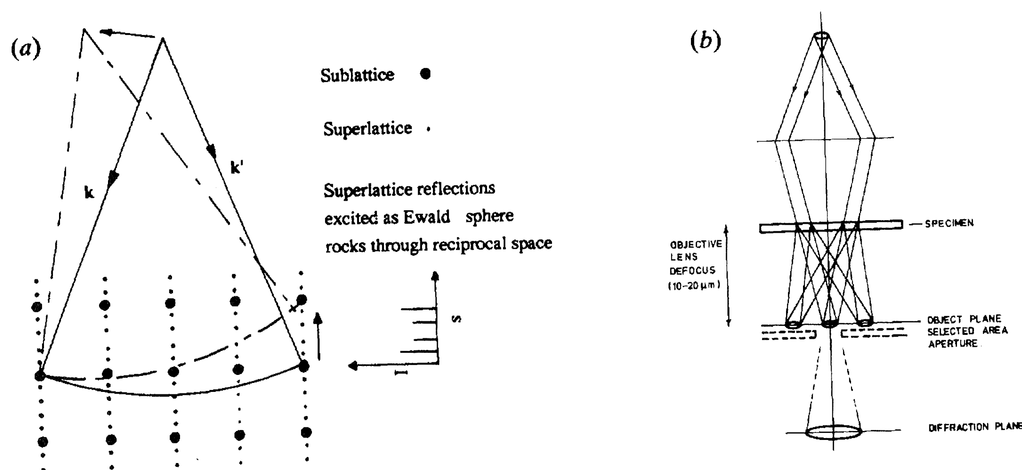

Figure 3. (*a*) Formation of an electron rocking curve in CBED/LACBED for a plan-view semiconductor superlattice. (*b*) A schematic of LACBED optics.

damage effects can be serious problems in certain instances. The technique may be applied to cross-sectional and plan-view specimens. For further details the above-mentioned reviews may be consulted. A few specific topics will be selected here for further comment.

One of the direct applications of CBED to cross sections of heterostructure interfaces or metal contacts is in the study of interfacial reactions. The symmetry and lattice parameter information available by use of this technique facilitate identification of known phases. More recently, methods have been developed which permit *ab initio* determination of the atomic arrangements in previously unknown phases (Vincent & Exelby 1991, 1993). For phases of modest dimensions (100 nm size) it is possible to locate atoms within the unit cell to an accuracy of about 1 pm. The accuracy of this technique relies on large angle diffraction to higher-order Laue zones. If, instead, attention is concentrated on the reflections close to the direct beam accurate information can be obtained about charge distributions (Bird & Saunders 1992).

The preparation of cross-sectional samples of semiconductors is time-consuming and results in relatively small interfacial regions which are thin enough for detailed examination. In the past few years a special development of CBED has been used to study interface structure in plan-view semiconductor samples. In general samples can be produced by back-thinning using selective chemical etches, resulting in near parallel-sided samples with areas 1 mm^2 or more which are sufficiently thin for detailed examination. In the plan-view geometry the absence of emerging interfaces means that sample relaxation is not a significant problem. This important development is discussed in the next section.

4. Large angle convergent beam diffraction (LACBED)

CBED has been used to profile composition and strain in a range of semiconductor multilayer structures. The information displayed across the diffraction disc for a

Downloaded from rsta.royalsocietypublishing.org

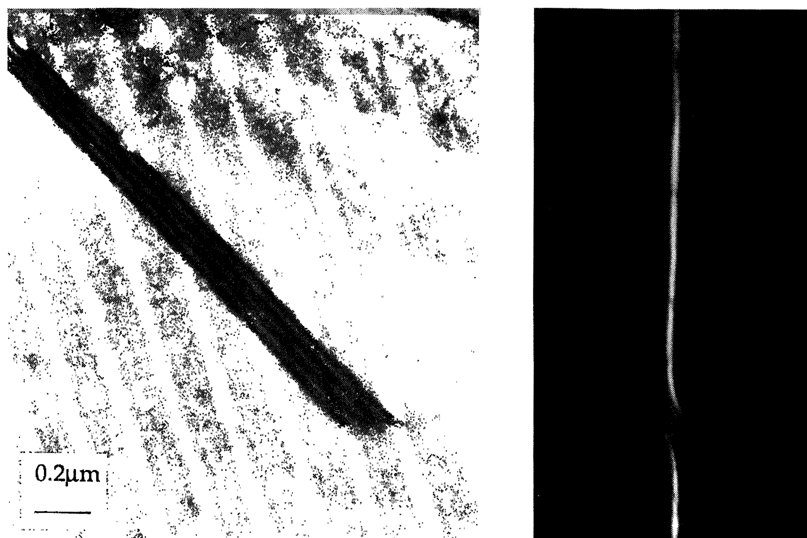

Figure 4. Stacking fault in a CdMnTe–CdTe bicrystal (left). A dark field 0, $\bar{1}\bar{0}$, 2 LACBED pattern which splits on bisecting the dislocation terminating the stacking fault (right). The number of subsidiary maxima, three, implies a value of $|\boldsymbol{g}\cdot\boldsymbol{b}| = 4$.

chosen reflection g represents an electron 'rocking curve' resolved approximately along the incident beam direction (figure 3*a*). In conventional CBED patterns, which are formed in the back-focal plane of the objective lens with the converging incident beam focused on the specimen, the rocking curve is limited to the Bragg angle (*ca.* 10^{-2} rad) to avoid overlapping of neighbouring discs. However, by bringing the incident beam to a focus out of the specimen plane, an aperture (the 'selected area' aperture) can be used to select a given diffracted beam to form a CBED pattern with only one diffraction disc (figure 3*b*). The rocking angle in this large angle CBED (LACBED) method can be increased to 10^{-1} rad or greater. Moreover, since the specimen is out of focus a shadow image of the illuminated area appears in the diffraction disc, the spatial resolution being determined by the minimum probe size (down to *ca.* 1–2 nm). That is, LACBED patterns display simultaneously real and reciprocal space information.

The LACBED method has emerged as a powerful means of analysing interfacial dislocations in semiconductors. In conventional imaging methods interfacial dislocations can be difficult to analyse owing to the dependence of dislocation strain fields on the mismatch in elastic constants across interfaces. In contrast, the essential details of LACBED images of dislocations depend on a geometrical criterion defined by the Burgers vector (Cherns & Preston 1986, 1989). Figure 4 shows an example where LACBED was used to analyse the nature of the threading dislocation bounding a stacking fault in CdMnTe–CdTe. The LACBED pattern shows that the 0, $\bar{1}\,\bar{0}$, 2 contour, which is unaffected by the stacking fault, dissociates on crossing the line of the threading dislocation. The value of $|g\cdot b| = 4$, consistent with a Burgers vector of Frank type $\frac{1}{3}\langle 111\rangle$, is determined simply by counting the number of image peaks seen as the contour crosses the dislocation; for further details the reader is referred to the papers noted above.

LACBED patterns from periodic multilayer structures display superlattice satellite peaks which are displaced from each fundamental diffracted beam along the growth

Downloaded from rsta.royalsocietypublishing.org

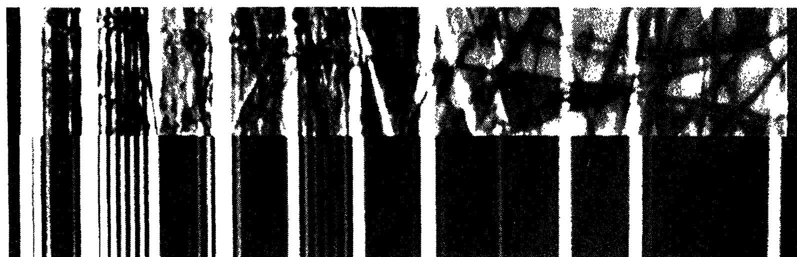

Figure 5. 200 dark field LACBED pattern from a 19.2 InP–11.1 nm $In_{0.53}Ga_{0.47}As$ superlattice in the range $0.03 < s < 0.4\ nm^{-1}$. Top, experimental; bottom, simulation; s increases left to right. (Courtesy of I. K. Jordan, unpublished work.)

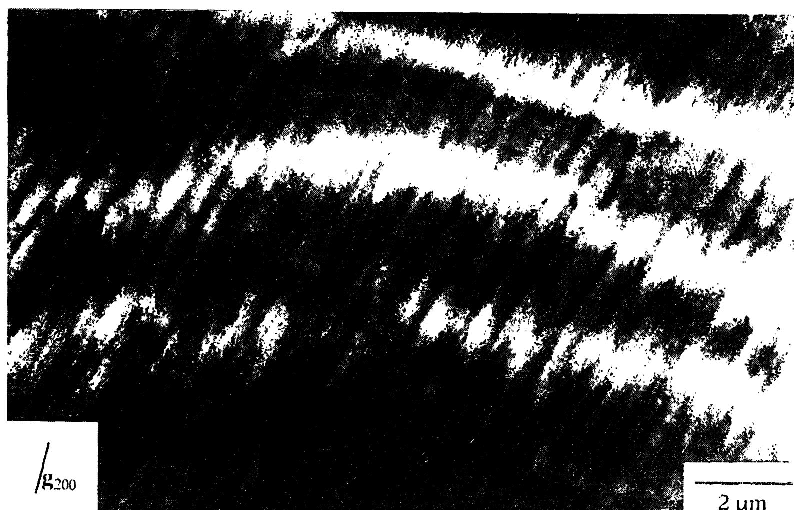

Figure 6. 200 dark field image of an InP–$In_{0.53}Ga_{0.47}As$–InP sample. Bright and dark bands represent changes in thickness of the $In_{0.53}Ga_{0.47}As$ quantum well, which has an average thickness of 5 nm. (Courtesy of I. K. Jordan, unpublished work.)

direction (figure 3). Figure 5 shows superlattice reflections in a 200 dark field LACBED pattern from a periodic 19.2 nm InP/11.1 nm $In_{0.53}Ga_{0.47}As$ multilayer. Only part of the diffraction disk is displayed containing superlattice reflections $n = 1$–12 on one side of the Bragg peak ($n = 0$). Although electron diffraction involves strong scattering, quite reasonable agreement is achieved here between experiment (top) and a kinematical simulation (bottom). In the kinematical approximation, which has been shown to apply with reasonable accuracy to the diffraction situation we are considering, the scattered amplitude A_g is given by

$$A_g = \int_0^t F_g(z) \exp[-2\pi i(sz + \boldsymbol{g} \cdot \boldsymbol{R})]\, dz, \tag{2}$$

where s is the deviation parameter ($= 0$ for the Bragg peak), $\boldsymbol{R}$ is any displacement field and z is the depth in a crystal of total thickness t. For a periodic multilayer of the type in figure 5, lattice matched and with no interface displacements ($\boldsymbol{R} = 0$), equation (2) predicts superlattice peaks at $\boldsymbol{g} \pm n\boldsymbol{q}$ where $|q| = D^{-1}$ where D is the

Downloaded from rsta.royalsocietypublishing.org

period. The superlattice peaks are in turn modulated by an envelope function given by

$$A_n = (D/\pi n)(\sin \pi n d_1/D)\,\Delta F_g, \tag{3}$$

where d_1 and d_2 are the thicknesses of the constituent layers ($D = d_1 + d_2$) and ΔF_g the difference in structure factor between the layers. In figure 6 the weakness of the satellites $n = 8, 11$ is explained by near minima in the envelope function (equation (3)).

LACBED patterns from periodic multilayers have been analysed by both kinematical and full dynamical treatments (see Cherns 1991; Cherns *et al.* 1991; Rossouw *et al.* 1991). Both approaches can give the period and the individual layer thicknesses to near monolayer precision. Local variations in both the period and the d_1/d_2 ratio have been monitored by observing spatial variations in the LACBED patterns (see Vincent *et al.* 1987; Cherns 1991). LACBED patterns from semiconductor multilayers have also been found to be a sensitive function of layer strains. The effect depends on the relative angle of rotation of the diffracted planes between adjacent layers, $\delta\theta$, given approximately by

$$\delta\theta = \tfrac{1}{2}\epsilon[(1+v)/(1-v)]\sin 2\theta, \tag{4}$$

where θ is the inclination of the planes to the growth plane, ϵ is the difference in strain between the layers and v is Poisson's ratio. Since electron diffraction enables us to examine diffraction from planes either affected or unaffected by strain ($\delta\theta$ finite or zero respectively), strain and composition profiles can be effectively separated. It has been shown that layer strains down to *ca.* 2×10^{-4} are detectable (Cherns *et al.* 1991).

The excellent visibility of superlattice reflections in LACBED patterns from periodic multilayers is due in part to the effective filtering of inelastic background achieved by the selected area aperture and in part to the fact that spatial averaging is minimized due to the small effective probe size (see earlier). The latter point implies that we could, in principle, separate interface diffuseness (e.g. due to interdiffusion) from the effects of interface roughness and sample bending. Calculations suggest that interface diffuseness on the 1–2 nm scale could indeed be studied by this method (see Cherns 1991). The excellent quality of LACBED patterns from semiconductors has also enabled us to study individual thin layers and single interfaces in great detail. Cherns *et al.* (1988) showed that thin (3 nm) quantum wells of GaAs in AlGaAs–GaAs–AlGaAs samples could be examined by LACBED. The method has been extended to study thin InGaAs quantum wells in InP–InGaAs–InP samples giving the local well thickness to within a monolayer and locating individual interface steps (Jordan *et al.* 1989, 1991). Although the effect of a thin embedded layer on the electron rocking curve increases with layer thickness, embedded layers down to only 1–2 monolayers thick can be detected. The sensitivity of the rocking curve to a single embedded layer suggests also that dark field images taken under appropriate diffracting conditions should be sensitive to the embedded layer thickness. This has been found to be the case (Jordan *et al.* 1989, 1991; Grigorieff *et al.* 1993) and an example is seen in figure 6, which shows alternate bright and dark bands of contrast where the thickness of an InGaAs quantum well embedded in InP varies locally. Such images give a detailed picture of interface topology at the atomic level.

Downloaded from rsta.royalsocietypublishing.org

5. Coherent electron diffraction (CED) and electron holography

A new development has occurred during the past year which holds out important prospects for the study of semiconductor interfaces by electron diffraction. This development is the ability to perform experiments by coherent electron diffraction, which record both the amplitudes and phases of the diffracted waves. In addition, there has been rapid growth in the closely related field of electron holography. Both these developments have been made possible by the commercial availability of stable field emission sources on transmission electron microscopes with excellent imaging and diffraction facilities.

Although the idea of coherent electron diffraction was developed about 20 years ago (Spence 1979), the results obtained, until recently, were of rather poor quality. In view of the potential ability to study local electron fields at semiconductor interfaces and in strained layer systems the new developments will be reviewed and some of the recent results presented.

To perform CED experiments good longitudinal (temporal) and lateral (spatial) coherence of the field emission source is required. The instrument used in the experiments reported here (a Hitachi HF2000) had a cold field emission source with an energy spread (FWHM) of 0.5 eV for a beam energy of 200 keV. This corresponds to a longitudinal coherence length of about 0.5 μm and wave packets composed of 4×10^5 waves.

A small probe size is also required (Spence & Cowley 1978). A good test for coherence is to investigate the intensity in the overlap region between two overlapping convergent beam discs. If this intensity is the sum of the two intensities of the separate discs, and is independent of the probe position, then the illumination is incoherent. If, however, the overlap intensity differs from the sum of the individual intensities, and is position-dependent, the illumination is coherent. It may be shown that for overlapping discs, separated by g, the probe focused on the specimen must have a diameter which is smaller than the appropriate plane spacing $2\pi/g$. The overlap intensity takes the form

$$I = A_1^2+A_2^2+2A_1A_2\cos(\phi_2-\phi_1+gx), \qquad (5)$$

where A_i and Φ_i are the amplitudes and phases of the ith diffracted beam and x measures the probe position relative to the crystal repeat $2\pi/g$ (Vine *et al.* 1992). As the probe is moved through a distance equal to the crystal repeat, this overlap intensity will go through one complete period of sinusoidal oscillation.

It may be useful to slightly over- or under-focus the probe relative to the specimen plane. Then, rather like the case of LACBED, there is a relationship between position in the overlap region of the CBED disc and position in the specimen. It follows that fringes will be observed which have a period dependent on the degree of under- or over-focusing and on orientation perpendicular to $\boldsymbol{g}$. The new expression for the overlap intensity becomes (Steeds *et al.* 1992)

$$I = A_1^2+A_2^2+2A_1A_2\cos\{\phi_2-\phi_1+g[x+(K_2-K_1)\Delta f/k]\}, \qquad (6)$$

where K_1 and K_2 are two different orientations in the overlap region, Δf is the amount of defocus and $k = 2\pi/\lambda$ is the electron wave number.

Fringes generated in this way have been demonstrated using various polytypes (6H, 15R, 4H) of SiC oriented along their $\langle 11\bar{2}0\rangle$ axes. The number of fringes increases with increase of defocus, up to a maximum determined by the lateral

PHILOSOPHICAL TRANSACTIONS OF THE ROYAL SOCIETY A MATHEMATICAL, PHYSICAL & ENGINEERING SCIENCES

Downloaded from rsta.royalsocietypublishing.org

coherence of the beam, which is thus determined to be approximately 30 nm. Careful study of these micrographs will reveal the different phasing of the reflections in different parts of the pattern. In the case of thin-enough crystals the diffracted amplitudes are equal to the structure factors and the fringes then give the relative phases of the structure factors. Further analysis of the results can be found in Steeds *et al.* (1992).

For an electron beam propagating in the z direction with $\boldsymbol{R}$ measured perpendicular to z, in an electric potential field $V(\boldsymbol{R}, z)$, the phase change introduced can be shown to be

$$\Delta\phi = \frac{\pi}{\lambda E_0}\int_{\text{path}} V(\boldsymbol{R}, z)\,\mathrm{d}z, \tag{7}$$

where E_0 is the beam energy.

Regions with electric fields along the beam direction have a large effect; fields perpendicular to the beam have no effect. Results based on these ideas have been obtained in low resolution, off-axis, electron holograms over a number of years by Pozzi, Merli and co-workers in Bologna (Merli *et al.* 1979; Matteucci *et al.* 1991; Frabboni *et al.* 1985). The challenge now is to explore the application of these new techniques of high spatial-resolution, coherent, electron diffraction to some of the many problems of current interest concerning semiconductor interfaces. Electric fields are sometimes held to be associated with extended, defects in semiconductors such as dislocations, stacking faults and twins. {111} grown III–V strained-layer structures have large internal electrical fields generated by the piezo-electric effect. δ-doped layers are inserted in III–V epilayers to introduce field-controlling band-offsets or Schottky barrier heights. It will be interesting to explore, in the future, what direct information can be obtained concerning some of these issues using CED or high resolution electron holography.

6. Spectroscopic techniques in TEM

There is a wide variety of spectroscopic techniques which are available in a modern TEM. These include energy dispersive X-ray (EDX) analysis, electron energy loss spectroscopy (EELS), Auger electron spectroscopy (AES) and cathodoluminescence (CL) spectroscopy. Three of these, EELS, EDX and AES, will receive no more than a mention here; neither have quite the spatial resolution required to study chemical profiles of interfaces, although the resolutions of both techniques now approach 2 nm (Isakozawa *et al.* 1990; Hembree 1992). They are invaluable for obtaining local chemical information at the 1% level.

At first sight cathodoluminescence spectroscopy would not appear to compete with the others in spatial resolution. We shall see that there is a sense in which it does. However, although not readily practised, there is a sense in which it is absolutely superior to the other spectroscopic techniques, in detecting and investigating very low doping and impurity levels, which singles it out for special mention here.

There are three main problems with performing CL experiments in a TEM. The first is the very low signal, the second is the need to cool the specimen and the third is the possibility of beam-dependent changes to the specimen. We shall discuss each of the points in turn.

The low signal is a consequence of the low rate of energy deposition in thin specimens and the ease with which the carriers created, when energy if deposited,

Downloaded from rsta.royalsocietypublishing.org

diffuse to the surfaces, to recombine non-radiatively. For high spatial resolution thin specimens are necessary to limit the carrier diffusion length and then even more surface recombination occurs. A very efficient system is required to capture as many of the available photons as possible (Roberts 1981).

To study the very informative near-edge emission from high quality semiconductors it is necessary if possible to obtain very low temperatures so that donors and acceptors are not thermally ionized and so that excitons not only form but are bound to impurities, dopants or defects. Even with a well-designed liquid helium stage the tortuous cooling path through a thin specimen, its mounting and parts of the specimen holder mean that it is unlikely that temperatures below 15 K will be achieved and that is not low enough for relatively small band gap semiconductors such as Si.

The term 'beam-dependent changes' covers a multitude of effects such as ion damage (ions often accompany the electron beam in a well-aligned microscope), electron displacement of atoms or ionization, contamination or passivation. Some of these effects are notoriously hard to control and are not well understood.

In spite of these difficulties some remarkable results have been achieved in TEM CL including low temperature monochrometer images with 50 nm spatial resolution (Wang *et al.* 1991). However, in favourable cases, much higher spatial resolution of detail can be achieved. It is fortunate that the plan view samples studied by LACBED are ideal for the CL technique. The two techniques can in fact be used on the same specimens with the same object in mind, investigation of interface sharpness. An electron beam incident on a selectively etched plan-view sample containing quantum wells will generate carriers throughout the specimen thickness, but the band gap discontinuities will cause these carriers to diffuse preferentially into the quantum wells, minimizing surface loss and causing strong quantum well luminescence. Where the quantum wells have plateaus large in comparison with the quantum well exciton size, the excitons when they emit photons will, on average, lie in quantum wells which are an integral number of layers wide. For each layer width there is a distinct emission line so that for high quality material a small number of narrow individual peaks is observed in the spatial region appropriate to the average well width (Milley *et al.* 1986; Bimberg *et al.* 1988; Steeds 1989). Such spectra, common in optical spectroscopy, can be quite informative in TEM CL experiments. Suppose there two peaks corresponding to regions $(n-1)$ and n layers thick. Then monochrometer images may be formed by adjusting a pass band to correspond to each of the emission peaks in turn. As expected, the resulting intensity maps are complimentary, where one is dark the other is bright and vice versa. This technique therefore allows the determination of plateau sizes of regions varying in thickness by just one monolayer. Interesting and useful though these results are they have to be interpreted with some caution, as emphasized by Warwick *et al.* (1990), because they necessarily involve averaging over the exciton dimensions and the results obtained are not easily compared with the results of HREM (see §2).

There are many other aspects of TEM CL which are of considerable interest in probing phenomena related to semiconductor interfaces. Dislocation and stacking-fault related luminescence effects may be studied directly, impurity distributions in alloy clustering effects can be mapped, quantum dots and quantum wires may be investigated in detail. For further details of this technique the interested reader is referred to Steeds (1992) as a general introduction and Wang *et al.* (1990) for quantum dots and Wang *et al.* (1993) for interfacial strains.

PHILOSOPHICAL TRANSACTIONS OF THE ROYAL SOCIETY A MATHEMATICAL, PHYSICAL & ENGINEERING SCIENCES

PHILOSOPHICAL TRANSACTIONS OF THE ROYAL SOCIETY A MATHEMATICAL, PHYSICAL & ENGINEERING SCIENCES

Downloaded from rsta.royalsocietypublishing.org

7. Conclusions

Transmission electron microscopy is a powerful technique for probing semiconductor interfaces. A wide variety of imaging, diffraction and spectroscopic techniques exists. Many of them are in a rapid state of development so that information can be obtained reliably at the near-atomic level.

We acknowledge frequent and stimulating interaction with colleagues, visitors, postdoctoral research assistants and Ph.D. students as the work, reviewed here, has developed in Bristol. We are also grateful for permission to use material as illustrations in this article taken from the work of researchers in Bristol. We further acknowledge the support of the Science and Engineering Research Council for several aspects of the work.

References

Bimberg, D., Christen, J., Fukunaga, T., Nakashima, H., Mars, D. E. & Miller, J. N. 1988 Direct imaging of the columnar structure of GaAs quantum wells. *Superlatt. Microstruct.* **4**, 257–263.

Bird, D. M. & Saunders, M. 1992 Sensitivity and accuracy of CBED pattern matching. *Ultramicroscopy* **45**, 241–251.

Cherns, D. & Preston, A. R. 1986 Convergent beam diffraction studies of crystal defects. In *Proc. 11th Int. Congress on Electron Microscopy*, Kyoto, Japan, vol. 2, pp. 1463–1464.

Cherns, D. & Preston, A. R. 1989 Convergent beam diffraction from interfaces, defects and multilayers. *J. Electron Microscope Technol.* **13**, 111–122.

Cherns, D., Jordan, I. K. & Vincent, R. 1988 Convergent beam electron diffraction from AlGaAs/GaAs single quantum wells. *Phil. Mag. Lett.* **58**, 45–51.

Cherns, D. 1991 Convergent beam diffraction and microscopy of single and multiple quantum well structures. *Inst. Phys. Conf. Ser.* no. 117, 549–558.

Cherns, D., Touaitia, R., Preston, A. R., Rossouw, C. J. & Houghton, D. C. 1991 Convergent beam diffraction studies of strain in Si/SiGe superlattices. *Phil. Mag.* A **64**, 597–612.

Chou, C. T., Hutchison, J. L., Casenove, M.-J., Cherns, D., Steeds, J. W., Ashenford, D. A. & Lunn, B. 1993 A new interfacial phase in ZnTe/(100) GaSb. In *Proc. Int. Conf. on microscopy of semiconducting materials, Oxford, April.*

Cowley, J. M. 1979 Coherent interference in convergent beam electron diffraction and shadow imaging. *Ultramicroscopy* **4**, 435–450.

Frabboni, S., Matteucci, G., Pozzi, G. & Vanzi, M. 1985 Electron holographic observations of the electrostatic field associated with thin reverse-biased *p–n* junctions. *Phys. Rev. Lett.* **55**, 2196–2199.

Grigorieff, N., Cherns, D., Yates, M. J., Hockly, M., Perrin, S. D. & Aylett, M. R. 1993 Electron microscopy of ultra-thin buried layers in InP and InGaAs. *Phil. Mag.* A. (In the press.)

Hembree, G. G. 1992 Auger electron spectroscopy at nanometer resolution. In *Proc. 50th Annual Meeting of the Electron Microscopy Society of America* (ed. G. W. Bailey, J. Bentley & J. A. Small), pp. 1476–1477. San Francisco Press.

Isakozawa, S., Sato, Y., Kashikura, Y., Kubo, T., Hashimoto, T., Takahashi, T., Ichihashi, M., Murakoshi, H., Kamino, T. & Ueki, Y. 1990 *Hitachi Instrument News* **19**, 9–14.

Jordan, I. K., Cherns, D., Grigorieff, N., Hockly, M., Spurdens, P. C., Aylett, M. R. & Scott, E. G. 1991 Convergent beam electron diffraction and microscopy of interface atomic steps in InP/InGaAs single quantum wells. *Inst. Phys. Conf. Ser.* no. 117, 563–568.

Jordan, I. K., Cherns, D., Hockly, M. & Spurdens, P. 1989 Convergent beam electron diffraction from InP/InGaAs single quantum wells. *Inst. Phys. Conf. Ser.* no. 100, 293–298.

Krivanek, O. L., Gubbens, A. J. & Dellby, N. 1991 Developments in EELS instrumentation for spectroscopy and imaging. *Microsc. Microanal. Microstruct.* **2**, 315–332.

Matteucci, G., Missiroli, G. F., Nichelatti, E., Migliori, A., Vanzi, M. & Pozzi, G. 1991 Electron holography of long range electric and magnetic fields. *J. appl. Phys.* **69**, 1835–1842.

Downloaded from rsta.royalsocietypublishing.org

Merli, P. G., Missiroli, G. F. & Pozzi, G. 1974 *p–n* junction observations by interference electron microscopy. *J. Microscopie* **21**, 11–20.

Miller, R. C., Tu, C. W., Sputz, S. K. & Kopf, R. F. 1986 *Appl. Phys. Lett.* **49**, 1245–1247.

Ourmazd, A., Baumann, F. H., Bode, M. & Kim, Y. 1990 Quantitative chemical lattice imaging: theory and practice. *Ultramicroscopy* **34**, 237–255.

Ourmazd, A., Taylor, D. W., Cunningham, J. & Tu, C. W. 1989 Chemical mapping of semiconductor interfaces at near-atomic resolution. *Phys. Rev. Lett.* **62**, 933–936.

Rackham, G. M. & Steeds, J. W. 1976 Convergent beam observations near boundaries and interfaces. In *EMAG 75 – Developments in Electron Microscopy and Analysis*, pp. 457–460. London: Academic Press.

Roberts, S. H. 1981 Cathodoluminescence of ZnS in the transmission electron microscope. In *Microscopy of Semiconducting Materials 1981: Inst. Phys. Conf. Ser.* no. 60 (ed. A. G. Cullis & D. C. Joy), pp. 377–380. Bristol: Institute of Physics.

Rossouw, C. J., Al-Khafaji, M., Cherns, D., Steeds, J. W. & Touaitia, R. 1991 A treatment of dynamical diffraction for multiply layered structures. *Ultramicroscopy* **35**, 229–236.

Spence, J. C. H. & Cowley, J. M. 1978 Lattice imaging in STEM. *Optik* **50**, 129–142.

Spence, J. C. H. & Zuo, J. M. 1992 *Electron microdiffraction* (358 pages.) New York and London: Plenum Press.

Spence, J. C. H. 1981 *Experimental high resolution electron microscopy*. Oxford: Clarendon Press.

Steeds, J. W. & Morniroli, J. P. 1992 Convergent beam and selected area electron diffraction. In *Minerals and reactions at the atomic scale – high resolution transmission electron microscopy*, ch. 2. Review in Mineralogy, vol. 27 (ed. P. R. Buseck), pp. 37–84. Chelsea Michigan: Mineralogical Society of America, Book Crafters. Inc.

Steeds, J. W. 1979 Convergent beam electron diffraction. In *Introduction to analytical electron microscopy* (ed. J. J. Hren, J. I. Goldstein & D. C. Joy), ch. 15, pp. 387–411. New York and London: Plenum Press.

Steeds, J. W. 1989 Performance and applications of a STEM–cathodoluminescence system. *Rev. Phys. appl. Colloq.* C6, **24**, 65–72.

Steeds, J. W. 1992 Cathodoluminescence. In *Encyclopedia of applied physics*, vol. 3, pp. 121–140. New York: VCH.

Steeds, J. W., Vincent, R., Vine, W. J., Spellward, P. & Cherns, D. 1992 Exploratory experiments in convergent beam electron diffraction. *Acta Microscopica* **1**, 1–13. (In abridged form in *Hitachi Instrument News* **24**, 3–11.)

Sung, C. & Williams, D. B. 1991 Principles and applications of convergent beam electron diffraction: a bibliography (1938–1990). *J. Elect. Micros. Technol.* **17**, 95–118.

Vincent, R. & Exelby, D. R. 1991 Structure of metastable Al–Ge phases determined by HOLZ Patterson transforms. *Phil. Mag. Lett.* **63**, 31–38.

Vincent, R. & Exelby, D. R. 1993 Structure of a metastable Al–Ga phase determined by large angle CBED patterns. *Phil. Mag.* A. (In the press.)

Vincent, R., Cherns, D., Bailey, S. J. & Morkoc, H. 1987 Structure of AlGaAs/GaAs multilayers imaged in superlattice reflections. *Phil. Mag. Lett.* **56**, 1–6.

Vincent, R., Vine, W. J., Midgley, P., Spellward, P. & Steeds, J. W. 1993 Coherent large angle CBED patterns in 6H SiC. *Ultramicroscopy*. (In the press.)

Vine, W. J., Vincent, R., Spellward, P. & Steeds, J. W. 1991 Observation of phase contrast in convergent beam electron diffraction patterns. *Ultramicroscopy* **41**, 423–428.

Wang, J. N., Steeds, J. W. & Arnot, H. 1990 The study of individual free-standing GaAs/AlGaAs quantum-dots by STEMCL. *Microsc. Microanal. Microstruct.* **1**, 241–246.

Wang, J., Steeds, J. W. & Henini, M. 1993 High resolution TEM-CL from the cross-sectional specimens of GaAs/AlGaAs QWs. *Colloq.* C6, *Suppl. J. Phys.* (III), **1**, 125–130.

Wang, J. N., Steeds, J. W. & Hopkinson, M. 1993 Microstructure and cathodoluminescence of MBE grown (001) $In_xGa_{1-x}P$/GaAs strained layer heterostructures. *Semicond. Sci. Technol.* (In the press.)

Warwick, C. A., Jan, W. Y., Ourmazd, A. & Harris, T. D. 1990 Does luminescence show semiconductor interfaces to be atomically smooth? *Appl. Phys. Lett.* **56**, 2666–2668.

PHILOSOPHICAL TRANSACTIONS OF THE ROYAL SOCIETY A MATHEMATICAL, PHYSICAL & ENGINEERING SCIENCES

PHILOSOPHICAL TRANSACTIONS OF THE ROYAL SOCIETY A
MATHEMATICAL, PHYSICAL & ENGINEERING SCIENCES
PHILOSOPHICAL TRANSACTIONS OF THE ROYAL SOCIETY A

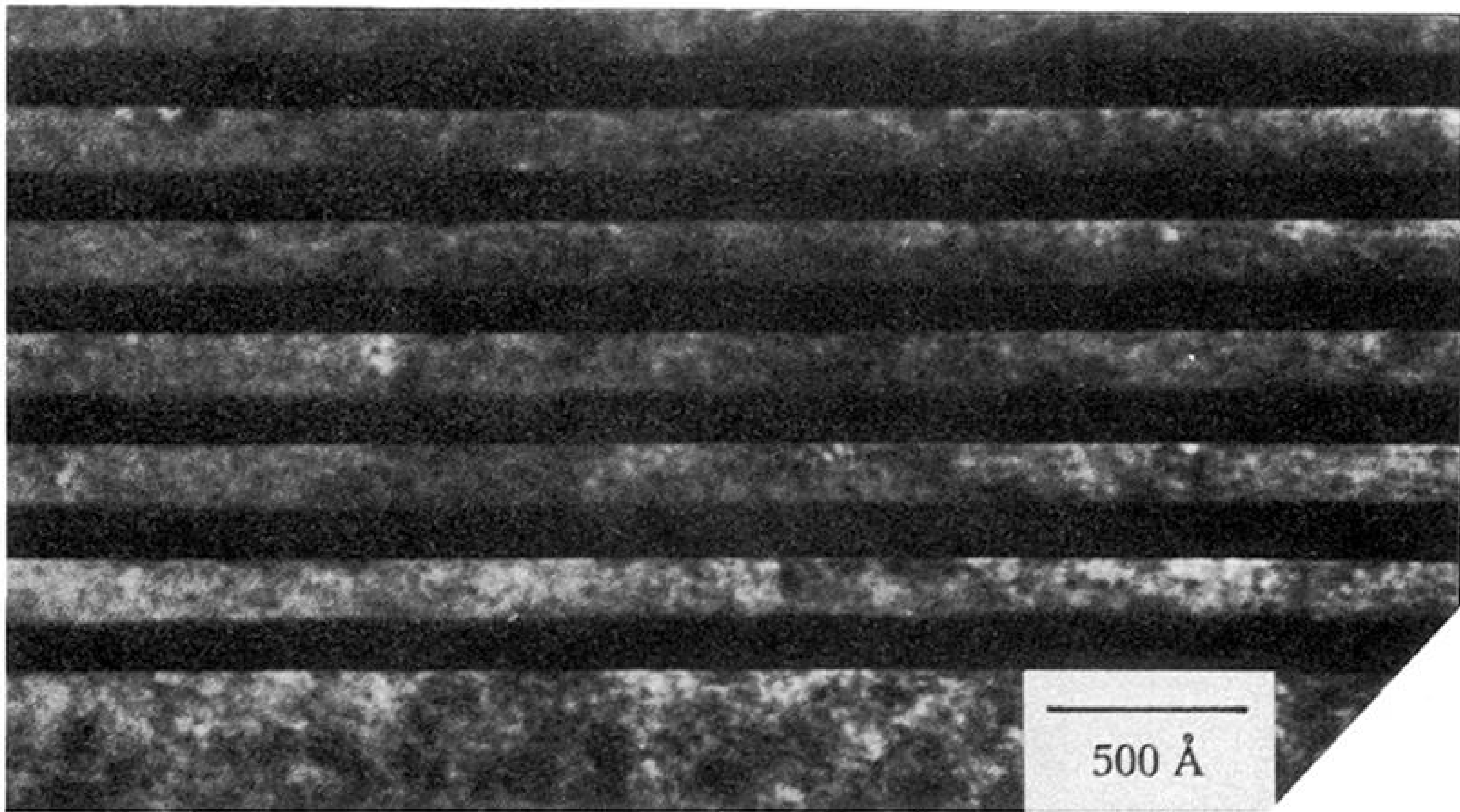

Figure 1. Dark field images in $g = 200$ of an $In_{0.53}Ga_{0.47}As/InP$ cross section. The growth direction is upwards and the InP layers are in strong contrast. (Courtesy of I. K. Jordan, unpublished work.)

PHILOSOPHICAL TRANSACTIONS OF THE ROYAL SOCIETY A MATHEMATICAL, PHYSICAL & ENGINEERING SCIENCES

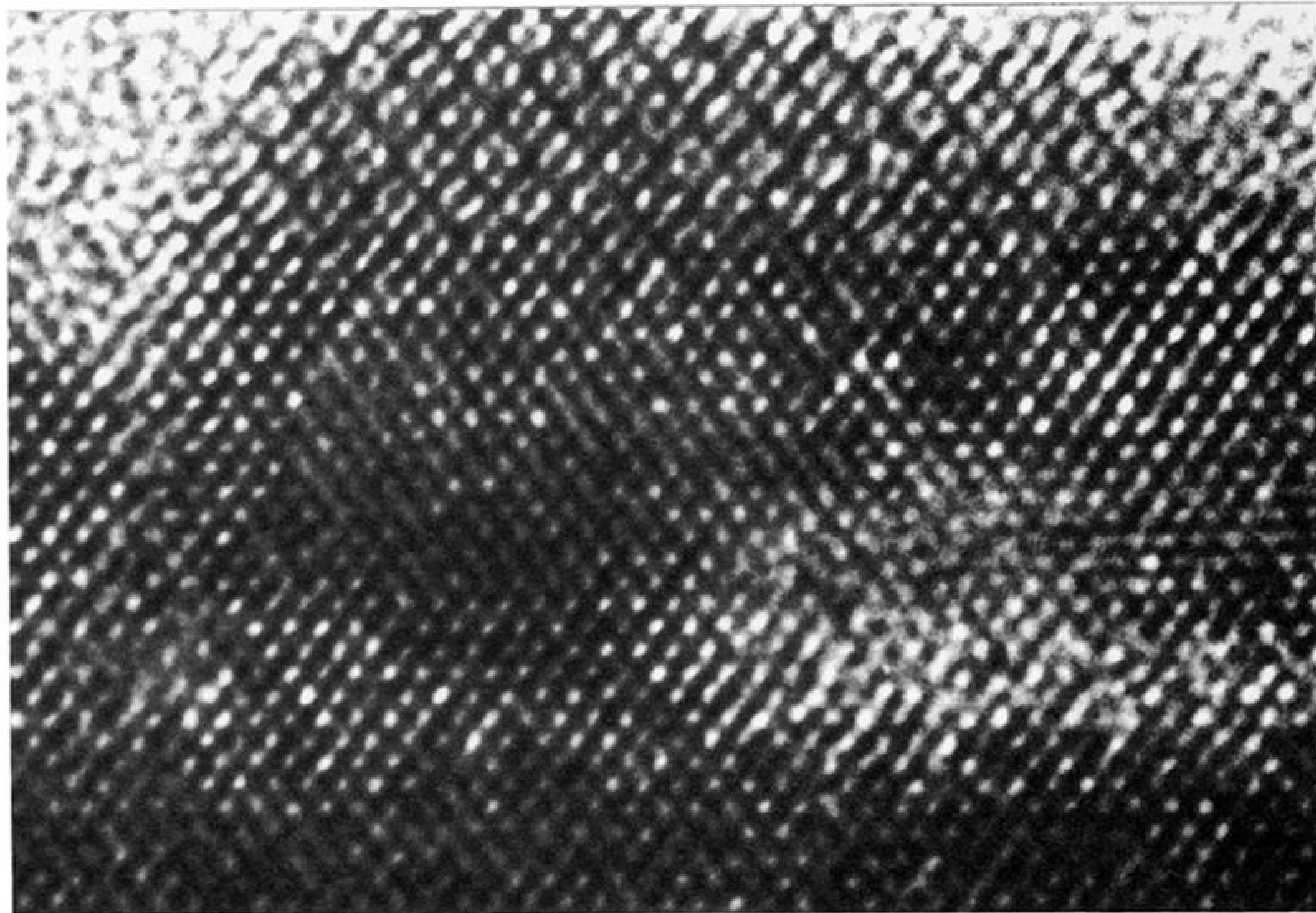

igure 2. (110) lattice image of a ZnTe–GaSb interface at a defocus of +56 nm. A new phase believed to be Ga_2Te_3 is arrowed. (Courtesy of C. T. Chou, unpublished work.)

PHILOSOPHICAL TRANSACTIONS OF THE ROYAL SOCIETY A MATHEMATICAL, PHYSICAL & ENGINEERING SCIENCES

Downloaded from rsta.royalsocietypublishing.org

PHILOSOPHICAL TRANSACTIONS OF THE ROYAL SOCIETY A MATHEMATICAL, PHYSICAL & ENGINEERING SCIENCES

PHILOSOPHICAL TRANSACTIONS OF THE ROYAL SOCIETY A MATHEMATICAL, PHYSICAL & ENGINEERING SCIENCES

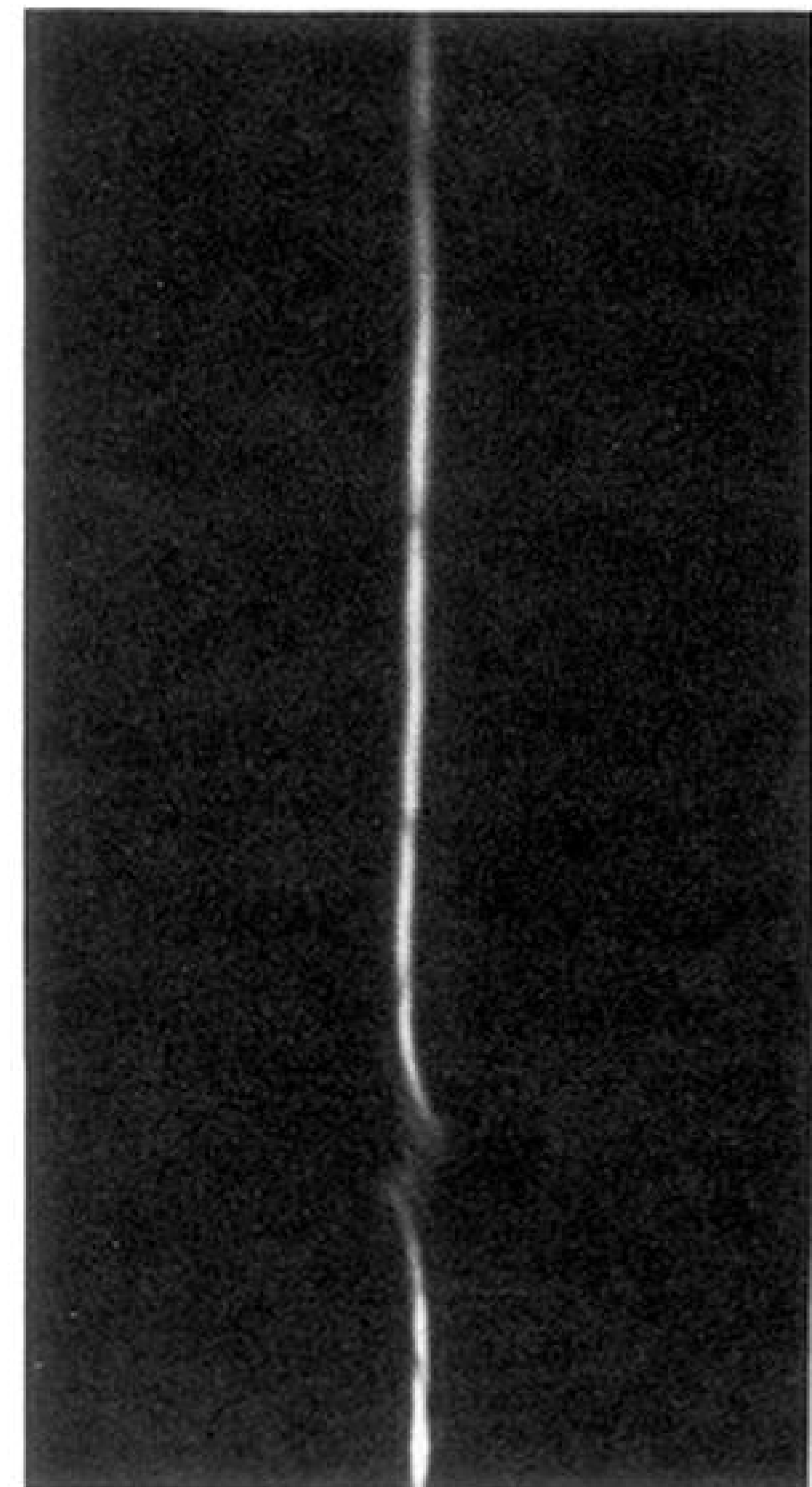

Figure 4. Stacking fault in a CdMnTe–CdTe bicrystal (left). A dark field 0, $\bar{1}\,\bar{0}$, 2 LACBED pattern which splits on bisecting the dislocation terminating the stacking fault (right). The number of subsidiary maxima, three, implies a value of $|\boldsymbol{g}\cdot\boldsymbol{b}| = 4$.

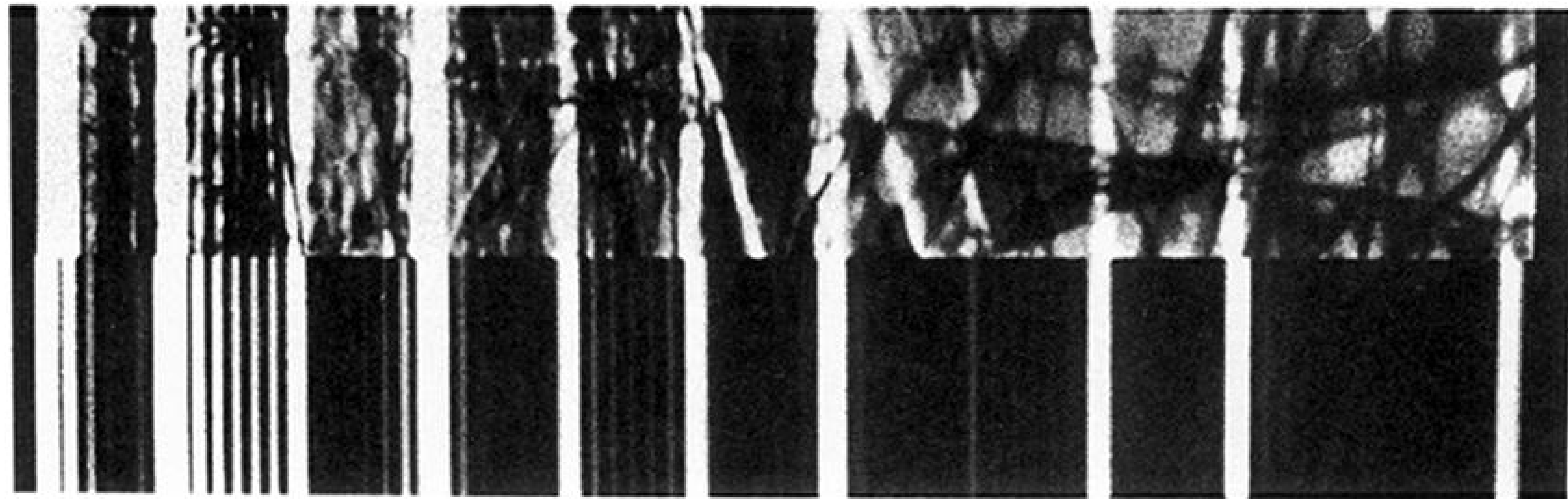

igure 5. 200 dark field LACBED pattern from a 19.2 InP–11.1 nm $In_{0.53}Ga_{0.47}As$ superlattice in the ange $0.03 < s < 0.4$ nm^{-1}. Top, experimental; bottom, simulation; s increases left to right. Courtesy of I. K. Jordan, unpublished work.)

PHILOSOPHICAL TRANSACTIONS OF THE ROYAL SOCIETY A MATHEMATICAL, PHYSICAL & ENGINEERING SCIENCES

PHILOSOPHICAL TRANSACTIONS OF THE ROYAL SOCIETY A MATHEMATICAL, PHYSICAL & ENGINEERING SCIENCES

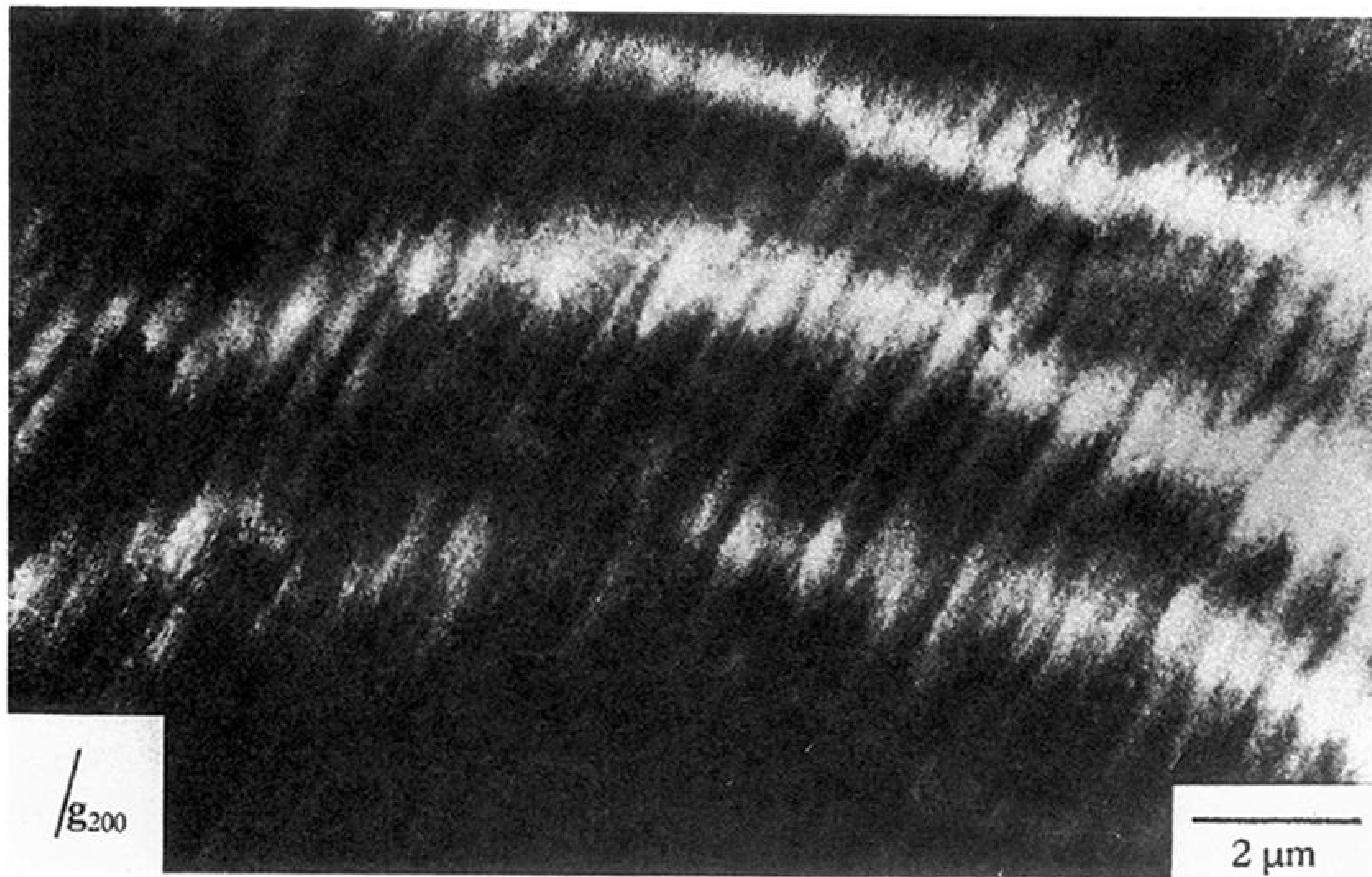

PHILOSOPHICAL TRANSACTIONS OF THE ROYAL SOCIETY A MATHEMATICAL, PHYSICAL & ENGINEERING SCIENCES

igure 6. 200 dark field image of an InP–$In_{0.53}Ga_{0.47}As$–InP sample. Bright and dark bands epresent changes in thickness of the $In_{0.53}Ga_{0.47}As$ quantum well, which has an average thickness f 5 nm. (Courtesy of I. K. Jordan, unpublished work.)